

# Equivalence of Pion Loops in Equal-Time and Light-Front Dynamics

Chueng-Ryong Ji

*Department of Physics, Box 8202, North Carolina State University,  
Raleigh, North Carolina 27692-8202*

W. Melnitchouk

*Jefferson Lab, 12000 Jefferson Avenue, Newport News, Virginia 23606*

A. W. Thomas

*Jefferson Lab, 12000 Jefferson Avenue, Newport News, Virginia 23606, and  
College of William and Mary, Williamsburg, Virginia 23187*

## Abstract

We demonstrate the equivalence of the light-front and equal-time formulations of pionic corrections to nucleon properties. As a specific example, we consider the self-energy  $\Sigma$  of a nucleon dressed by pion loops, for both pseudovector and pseudoscalar  $\pi NN$  couplings. We derive the leading and next-to-leading nonanalytic behavior of  $\Sigma$  on the light-front, and show explicitly their equivalence in the rest frame and infinite momentum frame in equal-time quantization, as well as in a manifestly covariant formulation.

## I. INTRODUCTION

From the approximate chiral symmetry of QCD it is known that the pion cloud of the nucleon plays a vital role in understanding the nucleon's long-range structure. It provides important corrections to static nucleon properties, such as the mass, magnetic moment and axial charge, and significantly influences its electric and magnetic charge distributions (for a review see Ref. [1]). At the quark level, the preferential coupling of a proton to a  $\pi^+$  and a neutron provides a natural explanation of the excess of  $\bar{d}$  quarks over  $\bar{u}$  in the proton sea [2], which has now been unambiguously established experimentally [3, 4, 5]. Since it is pseudoscalar, the emission of a pion from a nucleon also leads to a nontrivial redistribution of the spin and angular momentum of its quark constituents [6], which partially resolves the proton spin problem [7].

More recently, it has been established from the chiral expansion in QCD that pion cloud contributions to moments of twist-two parton distributions of the nucleon have a leading nonanalytic (LNA) behavior characteristic of Goldstone boson loops in chiral perturbation theory [8]. Since it is determined by the infrared properties of chiral loops, the LNA behavior is model-independent [9, 10, 11], and places the physics of the pion cloud on a firm footing in QCD.

In addition to the traditional studies of elastic form factors and parton distributions, there is a great deal of interest in the more recently defined generalized parton distributions (GPDs) [12]. As with the ordinary parton distribution functions, the physical interpretation of GPDs in terms of probability distributions is most natural on the light-front, or in the infinite momentum frame (IMF) of time-ordered perturbation theory (TOPT) [13], and one knows that here too chiral corrections can be very important. It is timely, therefore, to address the question of how to provide a consistent derivation of the chiral corrections to all of these observables on the light-front, and to explain in some detail the technical differences between these calculations on the light-front and either in equal-time or covariant formulations.

Historically the realization of chiral symmetry on the light-front has posed a serious theoretical challenge, and extreme care must usually be taken to avoid pathologies associated with so-called zero modes or spurious end-point singularities in light-front calculations. Indeed, the LNA behavior of twist-two matrix elements calculated in the meson cloud model

on the light-front (or in the IMF in equal-time quantization) with a pseudoscalar  $\pi N$  interaction [8] appeared to be in conflict with the results from covariant chiral perturbation theory [10, 11, 14, 15], which uses a pseudovector coupling. This led to questions being raised [10, 11] about the suitability of computing chiral corrections to hadronic matrix elements in meson cloud models on the light-front [13, 16, 17].

In other applications, the equivalence of light-front and manifestly covariant formalisms was demonstrated by Bakker *et al.* [18] for the vector two-point function and pseudoscalar charge form factor in  $1+1$  dimensions. (For an analogous discussion in QED see Ref. [19].) Using several different methods, it was shown [18] that spurious divergences can be avoided when performing loop integrals by properly taking into account contributions from the arc used to close the contour of integration at infinity. Furthermore, Sawicki [20] demonstrated for a scalar  $\phi^3$  theory that a smooth transition from equal-time perturbation theory to the light-front can be made without reference to the IMF limit.

In some cases, however, extreme care must be taken when computing the arc contributions, *viz.*, when one encounters so-called moving poles where the pole in the  $k^-$  momentum variable depends on the  $k^+$  integration variable. In particular, the contributions coming from the end points  $k^+ = 0$  and  $k^+ = p^+$  in the  $k^+$  range  $0 \leq k^+ \leq p^+$  must be taken into account as discussed in Ref. [18]. Without these end point contributions the complete equivalence between the light-front and manifestly covariant results cannot in general be demonstrated. It is amusing to see that the corrections we find restore covariance in the same way as the kinetic mass counter-term does in the work of Ref. [21].

In this paper we utilize some of these techniques to demonstrate the equivalence between equal-time and light-front dynamics for the interactions of nucleons with pions. We demonstrate that there is, in fact, no conflict between the results in equal-time, light-front or covariant frameworks, provided care is taken when performing loop integrations and if compares consistently the same theories (with pseudovector or pseudoscalar  $\pi N$  interactions). While a detailed analysis of the twist-two matrix elements in the different frameworks will be the subject of an upcoming work [22], here for illustration purposes we consider the specific example of the self-energy  $\Sigma$  of a nucleon dressed by a pion loop, and examine in particular the model-independent, nonanalytic behavior of  $\Sigma$  in the chiral limit.

In Sec. II we define the Lagrangian for the pseudovector (PV)  $\pi NN$  interaction, and introduce the self-energy for the dressing of a nucleon by a pion loop. Although the pseu-

doscalar (PS)  $\pi NN$  interaction does not preserve chiral symmetry (without the introduction of scalar fields), for completeness we also consider the pseudoscalar theory in Appendix A. We also present a convenient reparametrization of the momentum dependence in the loop integrations which allows the self-energy to be expressed entirely in terms of scalar propagators. The calculation of the self-energy within a covariant framework is presented in Sec. III using dimensional regularization. We derive results for the total  $\Sigma$ , including finite and divergent parts, but focus in particular on the structure of the model-independent, leading (and next-to-leading) nonanalytic contributions, and recover the standard results of chiral perturbation theory [23].

In Sec. IV we examine the self-energy in detail using time-ordered perturbation theory, both in the familiar rest frame of the nucleon, and in the IMF, where a probabilistic interpretation is applicable. The computation of  $\Sigma$  on the light-front, discussed in Sec. V, is closely related to the IMF formulation in equal-time dynamics. We verify that in all cases the correct results are obtained for the nonanalytic contributions. Finally, in Sec. VI we summarize our findings and outline future applications of the results. A presentation of the results for the self-energy with the PS interaction is given in Appendix A, and the LNA behavior of some relevant integrals is listed in Appendix B.

## II. DEFINITIONS

The lowest order  $\pi N$  interaction with a pseudovector coupling which is relevant for the self-energy is defined by the Lagrangian density [23, 24]

$$\mathcal{L} = \frac{f_{\pi NN}}{m_\pi} (\bar{\psi}_N \gamma^\mu \gamma_5 \vec{\tau} \psi_N) \cdot \partial_\mu \vec{\phi}_\pi, \quad (1)$$

where  $\psi_N$  and  $\vec{\phi}_\pi$  are the nucleon and pion fields,  $\vec{\tau}$  is the Pauli matrix operator in nucleon isospin space,  $m_\pi$  is the pion mass, and  $f_{\pi NN}$  is the pseudovector  $\pi NN$  coupling constant with  $f_{\pi NN}^2/4\pi \approx 0.08$ . The analogous pseudoscalar interaction is given in Appendix A. Often the PV coupling is expressed in terms of the PS coupling constant  $g_{\pi NN}$ ,

$$\frac{g_{\pi NN}}{2M} = \frac{f_{\pi NN}}{m_\pi}. \quad (2)$$

where  $M$  is the nucleon mass, with  $g_{\pi NN}^2/4\pi \approx 14.3$ . Using the Goldberger-Treiman relation the  $\pi NN$  coupling can also be expressed in terms of the axial vector charge of the nucleon,

$g_A$ ,

$$\frac{g_A}{f_\pi} = \frac{g_{\pi NN}}{M}, \quad (3)$$

where  $g_A = 1.267$  and  $f_\pi \approx 93$  MeV is the pion decay constant.

The self-energy operator  $\widehat{\Sigma}$  is given by [25]

$$\widehat{\Sigma} = i \left( \frac{g_{\pi NN}}{2M} \right)^2 \int \frac{d^4 k}{(2\pi)^4} (k \gamma_5 \vec{\tau}) \frac{i (\not{p} - \not{k} + M)}{(p - k)^2 - M^2 + i\epsilon} (\gamma_5 k \vec{\tau}) \frac{i}{k^2 - m_\pi^2 + i\epsilon} \quad (4)$$

and can be decomposed into scalar and vector components according to

$$\widehat{\Sigma} = \Sigma_v \not{p} + \Sigma_s. \quad (5)$$

Taking the matrix element of  $\widehat{\Sigma}$  between nucleon states, the self-energy (of mass shift) of a nucleon with momentum  $p$  dressed by a pion loop with momentum  $k$  is given by

$$\Sigma = \frac{1}{2} \sum_s \bar{u}(p, s) \widehat{\Sigma} u(p, s) = M \Sigma_v + \Sigma_s, \quad (6)$$

where the sum is over the nucleon spins  $s$ , and we have used the spinor normalization convention of Bjorken and Drell [26].

The expression in Eq. (4) can be simplified by writing the momentum variables in the numerator of the integrand (4) in terms of the pion and nucleon propagators  $D_\pi$  and  $D_N$ , where

$$D_\pi \equiv k^2 - m_\pi^2 + i\epsilon, \quad (7a)$$

$$D_N \equiv (p - k)^2 - M^2 + i\epsilon. \quad (7b)$$

Rearranging Eqs. (7), and dropping the irrelevant  $i\epsilon$  terms, one can make the replacements

$$k^2 \rightarrow D_\pi + m_\pi^2, \quad (8a)$$

$$p \cdot k \rightarrow \frac{1}{2} (D_\pi - D_N + m_\pi^2). \quad (8b)$$

After applying a trace over the nucleon spins and implementing these substitutions, the self-energy can be written as

$$\Sigma = -\frac{3ig_{\pi NN}^2}{4M^2} \int \frac{d^4 k}{(2\pi)^4} \frac{1}{2M} \left[ \frac{4M^2 k^2 + 2k^2 p \cdot k - 4(p \cdot k)^2}{D_\pi D_N} \right] \quad (9)$$

$$= -\frac{3ig_A^2}{4f_\pi^2} \int \frac{d^4 k}{(2\pi)^4} \frac{1}{2M} \left[ 4M^2 \left( \frac{m_\pi^2}{D_\pi D_N} + \frac{1}{D_N} \right) + \frac{2p \cdot k}{D_\pi} \right], \quad (10)$$

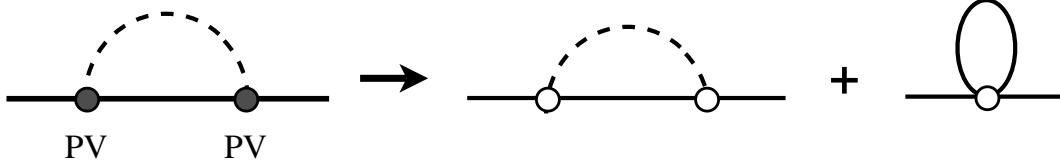


FIG. 1: Reduction of the self-energy in the pseudovector theory to an effective theory of “scalar nucleons” and pions (denoted by the open blobs at the vertices).

where in (10) we have used the Goldberger-Treiman relation (3). Note that because the term in Eq. (10) proportional to  $p \cdot k$  is odd in the pion momentum  $k$ , it will integrate to zero, provided the ultra-violet regulator does not introduce additional dependence on  $p \cdot k$ . In any case, this should not affect the infrared behavior of the integrand, and hence not affect the chiral behavior.

The individual scalar and vector contributions to the self-energy are given by

$$\Sigma_v = -\frac{3ig_A^2}{4f_\pi^2} \int \frac{d^4k}{(2\pi)^4} \left[ \frac{1}{D_N} + \frac{m_\pi^2}{D_\pi D_N} + \frac{1}{M^2} \frac{p \cdot k}{D_\pi} \right], \quad (11)$$

$$\Sigma_s = -\frac{3ig_A^2}{4f_\pi^2} \int \frac{d^4k}{(2\pi)^4} M \left[ \frac{1}{D_N} + \frac{m_\pi^2}{D_\pi D_N} \right]. \quad (12)$$

Interestingly, provided that the  $p \cdot k$  term in the vector self-energy does not contribute, the contributions to the total self-energy from the vector and scalar components are identical,

$$M\Sigma_v = \Sigma_s = \frac{1}{2} \Sigma. \quad (13)$$

This is not the case, however, for a pseudoscalar theory, as we discuss in Appendix A.

We can interpret the expression in Eq. (10) as a reduction of the pseudovector theory to an effective theory of “scalar nucleons” [27] and pions, involving a scalar self-energy and nucleon tadpole diagrams, as in Fig. 1. In the following sections we compute the self-energy  $\Sigma$  in several ways, including a direct manifestly covariant computation using dimensional regularization, in equal-time dynamics, both in the rest frame and in the infinite momentum frame, and on the light-front.

### III. COVARIANT FORMULATION WITH DIMENSIONAL REGULARIZATION

The self-energy can be evaluated in a manifestly covariant manner using dimensional regularization to regulate the ultra-violet divergence in the integral. We can compute the

self-energy covariantly by either integrating the full expression in Eq. (9) or the reduced result in Eq. (10). Since the latter is more straightforward, we present results calculated from the two propagator terms in (10) (the  $p \cdot k/D_\pi$  term integrates to zero), although we have verified that identical results are obtained with both expressions.

For the  $1/D_\pi D_N$  term, the product of the pion and nucleon propagators can be reduced using the Feynman parametrization

$$\frac{1}{D_\pi D_N} = \frac{1}{D_\pi - D_N} \left( \frac{1}{D_N} - \frac{1}{D_\pi} \right) \quad (14a)$$

$$= \int_0^1 dx \frac{1}{(xD_\pi + (1-x)D_N)^2}. \quad (14b)$$

Changing variables to  $k \rightarrow k' = k - (1-x)p$ , the denominator in the self-energy can be written as

$$xD_\pi + (1-x)D_N = k'^2 + D_{\text{cov}} + i\epsilon, \quad (15)$$

where

$$D_{\text{cov}} = -(1-x)^2 M^2 - x m_\pi^2. \quad (16)$$

Performing a Wick rotation to Euclidean space, the integral over the pion and nucleon propagators in  $d = 4 - 2\varepsilon$  dimensions, in the limit  $\varepsilon \rightarrow 0$ , can then be written as

$$\int d^d k \frac{1}{D_\pi D_N} = -i\pi^2 \left( \gamma + \log \pi - \frac{1}{\varepsilon} + \int_0^1 dx \log \frac{(1-x)^2 M^2 + x m_\pi^2}{\mu^2} + \mathcal{O}(\varepsilon) \right), \quad (17)$$

where  $\mu$  is a mass parameter introduced to give the correct mass dimensions in  $d$  dimensions,  $\Gamma(\varepsilon) = 1/\varepsilon - \gamma + \mathcal{O}(\varepsilon)$ , and  $\gamma \approx 0.577$  is Euler's constant. For the integral over the tadpole-like  $1/D_N$  term, we find

$$\int d^d k \frac{1}{D_N} = -i\pi^2 M^2 \left( \gamma + \log \pi - \frac{1}{\varepsilon} + \log \frac{\mu^2}{M^2} + \mathcal{O}(\varepsilon) \right), \quad (18)$$

where we have used the recurrence relation for the  $\Gamma$  function,  $\Gamma(\varepsilon - 1) = \Gamma(\varepsilon)/(\varepsilon - 1)$ . The infinitesimal parameter  $\varepsilon$  is set to zero at the end of the calculation, leading to singular results for the integrals, which in principle can be absorbed into counter-terms when computing observables. However, our concern here is the finite part of the integrals, and in particular the LNA behavior of  $\Sigma$ .

Combining the results in Eqs. (17) and (18), the self-energy becomes

$$\begin{aligned}\Sigma_{\text{cov}} = & -\frac{3g_A^2 M}{32\pi^2 f_\pi^2} \left\{ \left( \gamma + \log \pi - \frac{1}{\varepsilon} + \log \frac{M^2}{\mu^2} \right) (M^2 + m_\pi^2) - M^2 - 2m_\pi^2 \right. \\ & + \frac{m_\pi^3 \sqrt{4M^2 - m_\pi^2}}{M^2} \left( \tan^{-1} \frac{m_\pi}{\sqrt{4M^2 - m_\pi^2}} + \tan^{-1} \frac{2M^2 - m_\pi^2}{m_\pi \sqrt{4M^2 - m_\pi^2}} \right) \\ & \left. + \frac{m_\pi^4}{2M^2} \log \frac{m_\pi^2}{M^2} \right\}.\end{aligned}\quad (19)$$

It is remarkable that a closed form exists for the complete result of the self-energy, even in the relativistic formulation (see also Refs. [28, 29]). Expanding  $\Sigma_{\text{cov}}$  in powers of  $m_\pi/M$  and isolating the nonanalytic terms (namely, ones which are odd powers or logarithms of  $m_\pi$ ), the LNA behavior as  $m_\pi \rightarrow 0$  is given by

$$\Sigma_{\text{cov}}^{\text{LNA}} = -\frac{3g_A^2}{32\pi f_\pi^2} \left( m_\pi^3 + \frac{1}{2\pi} \frac{m_\pi^4}{M} \log m_\pi^2 + \mathcal{O}(m_\pi^5) \right), \quad (20)$$

where in addition to the  $\mathcal{O}(m_\pi^3)$  term, which agrees with the established results from chiral perturbation theory [23], for completeness we have also kept the next order,  $\mathcal{O}(m_\pi^4 \log m_\pi^2)$ , nonanalytic term. This is not the complete contribution to this order, however, as there exists an  $\mathcal{O}(m_\pi^4 \log m_\pi^2)$  term arising from diagrams with a pion loop accompanied by a  $\Delta$  intermediate state [30]. In fact, since this contribution depends on  $1/(M_\Delta - M)$ , where  $M_\Delta$  is the mass of the  $\Delta$ , rather than on  $1/M$  as in Eq. (20), it will give the next-to-leading contribution in the heavy baryon limit. Note also that because the  $1/D_N$  term in Eq. (10) is independent of  $m_\pi$ , it does not contribute to the nonanalytic behavior of  $\Sigma$ , which is solely determined by the  $1/D_\pi D_N$  term.

#### IV. EQUAL-TIME DYNAMICS

While the covariant calculation in the previous section is straightforward, it is instructive to examine the relative contributions to the self-energy from the different time orderings of the intermediate state. This can be realized using time-ordered perturbation theory, in which the pion and nucleon propagators are split up into their positive and negative energy poles. The relative contributions will naturally depend on the frame of reference, and we consider two commonly used examples, namely, the nucleon rest frame and the infinite momentum frame. Here the 4-dimensional integrals are computed by first performing the integrations over the energy  $k_0$ . The 3-momentum integration over  $\mathbf{k}$  will generally be divergent, so in



order to regularize the integrals we employ a 3-momentum cut-off on  $|\mathbf{k}|$ . The LNA behavior of the self-energy, which is the primary focus of this work, will of course be independent of the details of the ultraviolet regularization.

### A. Nucleon Rest Frame

The computation of the self-energy in the nucleon rest frame is most straightforward in terms of the reduced expression for  $\Sigma$  in Eq. (10). In contrast to the standard expression in Eq. (9) involving pion momenta in the numerator, the self-energy expressed solely through pion and nucleon propagators does not receive contributions from the arc at infinity when performing the  $k_0$  integration. The results are of course identical if one uses the original expression (9), although as we demonstrate below, in that case one must consider both pole terms and nonzero arc contributions.

Consider first the  $1/D_\pi D_N$  term, which when expanded into positive and negative energy components can be written

$$\int d^4k \frac{1}{D_\pi D_N} = \int d^3\mathbf{k} \int_{-\infty}^{\infty} dk_0 \frac{1}{(-2)(\omega_k - i\epsilon)} \left( \frac{1}{k_0 - \omega_k + i\epsilon} - \frac{1}{k_0 + \omega_k - i\epsilon} \right) \times \frac{1}{2(E' - i\epsilon)} \left( \frac{1}{k_0 - E + E' - i\epsilon} - \frac{1}{k_0 - E - E' + i\epsilon} \right), \quad (21)$$

where in the rest frame the target nucleon has energy  $E = M$ , the recoil nucleon energy is  $E' = \sqrt{\mathbf{k}^2 + M^2}$  and the pion energy is  $\omega_k = \sqrt{\mathbf{k}^2 + m_\pi^2}$ . Multiplying out the terms in the parentheses in Eq. (21), the resulting  $k_0$  integral has four contributions:

- $\Sigma_{\text{ET}}^{(+-)}$ : pion pole in the lower half-plane ( $\omega_k - i\epsilon$ ) and nucleon pole in the upper half-plane ( $E - E' + i\epsilon$ );
- $\Sigma_{\text{ET}}^{(-+)}$ : pion pole in the upper half-plane ( $-\omega_k + i\epsilon$ ) and nucleon pole in the lower half-plane ( $E + E' - i\epsilon$ );
- $\Sigma_{\text{ET}}^{(++)}$ : pion pole in the lower half-plane ( $\omega_k - i\epsilon$ ) and nucleon pole in the lower half-plane ( $E + E' - i\epsilon$ );
- $\Sigma_{\text{ET}}^{(--)}$ : pion pole in the upper half-plane ( $-\omega_k + i\epsilon$ ) and nucleon pole in the upper half-plane ( $E - E' + i\epsilon$ ),

where the superscripts  $(\pm\pm)$  refer to the signs of  $k_0$  in the pion and nucleon parts of the energy denominators, respectively. Note that the contribution  $\Sigma_{\text{ET}}^{(+-)}$  corresponds to the positive energy diagram, while  $\Sigma_{\text{ET}}^{(-+)}$  is the so-called “Z-graph”. Since the terms  $\Sigma_{\text{ET}}^{(++)}$  and  $\Sigma_{\text{ET}}^{(--)}$  have both poles in the same half-plane, one can choose the contour of integration to render their residues zero. However, in addition to the residues of the poles, the contour integrations also contain contributions from the arc at infinity, which must be subtracted,

$$\int_{-\infty}^{\infty} = \oint_C - \int_{\text{arc}} . \quad (22)$$

One can verify that closing the contour  $C$  in either the upper or lower half-plane gives the same results for  $\Sigma_{\text{ET}}^{(+-)}$  and  $\Sigma_{\text{ET}}^{(-+)}$ . For  $\Sigma_{\text{ET}}^{(++)}$  the contour can be chosen in the upper half-plane and for  $\Sigma_{\text{ET}}^{(--)}$  in the lower half-plane to exclude the pole contributions. From the powers of the energy  $k_0$  in the numerator and denominators in Eq. (21), however, one sees that the arc contributions will vanish at infinity. Performing the  $k_0$  integration, the four contributions to the self-energy then become

$$\Sigma_{\text{ET}}^{(+-)} = -\frac{3g_A^2 M}{16\pi^3 f_\pi^2} \int \frac{d^3 \mathbf{k}}{2E'} \frac{m_\pi^2}{2\omega_k} \left( \frac{1}{M - E' - \omega_k} \right), \quad (23a)$$

$$\Sigma_{\text{ET}}^{(-+)} = +\frac{3g_A^2 M}{16\pi^3 f_\pi^2} \int \frac{d^3 \mathbf{k}}{2E'} \frac{m_\pi^2}{2\omega_k} \left( \frac{1}{M + E' + \omega_k} \right), \quad (23b)$$

$$\Sigma_{\text{ET}}^{(++)} = 0, \quad (23c)$$

$$\Sigma_{\text{ET}}^{(--)} = 0. \quad (23d)$$

While it does not contribute to the LNA behavior of  $\Sigma$ , for completeness we consider also the  $1/D_N$  term in Eq. (10). Closing the  $k_0$  contour integration in either the upper or lower half-planes, the integral can be written

$$\begin{aligned} \int d^4 k \frac{1}{D_N} &= \int d^3 \mathbf{k} \int_{-\infty}^{\infty} dk_0 \frac{1}{(k_0 - E - E' + i\epsilon)(k_0 - E + E' - i\epsilon)} \\ &= -i\pi \int d^3 \mathbf{k} \frac{1}{E'}. \end{aligned} \quad (24)$$

Combining all the contributions, the total self-energy in the nucleon rest frame is

$$\Sigma_{\text{ET}} = -\frac{3g_A^2 M}{16\pi^3 f_\pi^2} \int \frac{d^3 \mathbf{k}}{2E'} \frac{1}{2\omega_k} \left( \frac{4\mathbf{k}^2 \omega_k + 2E'(\mathbf{k}^2 + \omega_k^2)}{(E' + \omega_k)^2 - M^2} \right). \quad (25)$$

The  $d^3 \mathbf{k}$  integration can be performed using spherical polar coordinates, with a high-

momentum cut-off  $\Lambda$  on  $|\mathbf{k}|$ , yielding the final result for the self-energy,

$$\begin{aligned}\Sigma_{\text{ET}} = & -\frac{3g_A^2 M}{32\pi^2 f_\pi^2} \left\{ 2\Lambda^2 + M^2 + (M^2 + m_\pi^2) \log \frac{M^2}{4\Lambda^2} \right. \\ & + \frac{m_\pi^3 \sqrt{4M^2 - m_\pi^2}}{M^2} \left( \tan^{-1} \frac{m_\pi}{\sqrt{4M^2 - m_\pi^2}} + \tan^{-1} \frac{2M^2 - m_\pi^2}{m_\pi \sqrt{4M^2 - m_\pi^2}} \right) \\ & \left. + \frac{m_\pi^4}{2M^2} \log \frac{m_\pi^2}{M^2} \right\}. \quad (26)\end{aligned}$$

We observe that the  $m_\pi$ -dependent terms in Eq. (26) are identical to those in the covariant calculation of  $\Sigma$  in Eq. (19), with the only differences appearing in terms that are analytic in  $m_\pi$  or which depend on the ultraviolet regulator. Not surprisingly, therefore, expanding  $\Sigma_{\text{ET}}$  in powers of  $m_\pi/M$ , the LNA structure in the chiral limit is

$$\Sigma_{\text{ET}}^{\text{LNA}} = -\frac{3g_A^2}{32\pi f_\pi^2} \left( m_\pi^3 + \frac{1}{2\pi} \frac{m_\pi^4}{M} \log m_\pi^2 + \mathcal{O}(m_\pi^5) \right), \quad (27)$$

which is consistent with the covariant result in Eq. (20). Note that the  $\mathcal{O}(m_\pi^3)$  term in Eq. (27) arises entirely from  $\Sigma_{\text{ET}}^{(+-)}$ , while the  $\mathcal{O}(m_\pi^4 \log m_\pi^2)$  term receives contributions from both the positive energy and Z-graphs,

$$\Sigma_{\text{ET}}^{(+-)\text{LNA}} = -\frac{3g_A^2}{32\pi f_\pi^2} \left( m_\pi^3 + \frac{3}{4\pi} \frac{m_\pi^4}{M} \log m_\pi^2 + \mathcal{O}(m_\pi^5) \right), \quad (28a)$$

$$\Sigma_{\text{ET}}^{(-+)\text{LNA}} = -\frac{3g_A^2}{32\pi f_\pi^2} \left( -\frac{1}{4\pi} \frac{m_\pi^4}{M} \log m_\pi^2 + \mathcal{O}(m_\pi^5) \right), \quad (28b)$$

so that combined they reproduce the LNA behavior in Eq. (27).

Had we worked from the original expression for the self-energy in Eq. (9),

$$\begin{aligned}\Sigma_{\text{ET}} = & -\frac{3ig_{\pi NN}^2}{4M^2} \frac{1}{(2\pi)^4} \int d^3\mathbf{k} \int_{-\infty}^{\infty} dk_0 \frac{k_0^3 - k_0 \mathbf{k}^2 - 2M \mathbf{k}^2}{(-2)(\omega_k - i\epsilon)2(E' - i\epsilon)} \\ & \times \left( \frac{1}{k_0 - \omega_k + i\epsilon} - \frac{1}{k_0 + \omega_k - i\epsilon} \right) \left( \frac{1}{k_0 - E + E' - i\epsilon} - \frac{1}{k_0 - E - E' + i\epsilon} \right), \quad (29)\end{aligned}$$

then the contributions from the corresponding four cross products would be

$$\Sigma'_{\text{ET}}{}^{(+ -)} = -\frac{3g_A^2}{32\pi^3 f_\pi^2} \int \frac{d^3\mathbf{k}}{2E'} \frac{1}{2\omega_k} \left\{ \frac{(M - E')^3 + \omega_k^3 - \mathbf{k}^2(5M - E' + \omega_k)}{2(M - E' - \omega_k)} - \frac{iR_\infty}{\pi}(M - E' + \omega_k) + \mathcal{O}(1/R_\infty) \right\}, \quad (30a)$$

$$\Sigma'_{\text{ET}}{}^{(- +)} = -\frac{3g_A^2}{32\pi^3 f_\pi^2} \int \frac{d^3\mathbf{k}}{2E'} \frac{1}{2\omega_k} \left\{ \frac{\omega_k^3 - (M + E')^3 - \mathbf{k}^2(-5M - E' + \omega_k)}{2(M + E' + \omega_k)} - \frac{iR_\infty}{\pi}(M + E' - \omega_k) + \mathcal{O}(1/R_\infty) \right\}, \quad (30b)$$

$$\Sigma'_{\text{ET}}{}^{(++)} = -\frac{3g_A^2}{32\pi^3 f_\pi^2} \int \frac{d^3\mathbf{k}}{2E'} \frac{1}{2\omega_k} \left\{ \frac{1}{2} [\omega_k^2 - \mathbf{k}^2 + \omega_k(M + E') + (M + E')^2] + \frac{iR_\infty}{\pi}(M + E' + \omega_k) + \mathcal{O}(1/R_\infty) \right\}, \quad (30c)$$

$$\Sigma'_{\text{ET}}{}^{(--)} = -\frac{3g_A^2}{32\pi^3 f_\pi^2} \int \frac{d^3\mathbf{k}}{2E'} \frac{1}{2\omega_k} \left\{ \frac{1}{2} [\mathbf{k}^2 - \omega_k^2 + \omega_k(M - E') - (M - E')^2] + \frac{iR_\infty}{\pi}(M - E' - \omega_k) + \mathcal{O}(1/R_\infty) \right\}. \quad (30d)$$

Here  $R_\infty$  is the magnitude of the energy  $k_0$  parametrized for the arc contribution,  $k_0 = R_\infty e^{\pm i\theta}$ , with  $\theta$  ranging from 0 to  $\pi$ , for contours closed in the upper or lower half-planes, respectively. In contrast to Eqs. (23), the terms  $\Sigma'_{\text{ET}}{}^{(++)}$  and  $\Sigma'_{\text{ET}}{}^{(--)}$  are nonzero, with  $\mathcal{O}(R_\infty)$  contributions arising from the arc at infinity. Remarkably, while each individual term in Eqs. (30) contains a divergent piece from the arc as  $R_\infty \rightarrow \infty$ , the total  $\mathcal{O}(R_\infty)$  contribution vanishes once all of the terms are summed. One can verify that adding the four terms in Eqs. (30) leads to the same result for the total self-energy  $\Sigma_{\text{ET}}$  as in Eq. (26).

The nonanalytic behavior of the individual components of the self-energy in Eqs. (30) is given by:

$$\Sigma'_{\text{ET}}{}^{(+ -)\text{LNA}} = -\frac{3g_A^2}{32\pi f_\pi^2} \left( m_\pi^3 + \frac{13}{16\pi} \frac{m_\pi^4}{M} \log m_\pi^2 \right), \quad (31a)$$

$$\Sigma'_{\text{ET}}{}^{(-+)\text{LNA}} = -\frac{3g_A^2}{32\pi f_\pi^2} \left( -\frac{1}{2\pi} M m_\pi^2 \log m_\pi^2 - \frac{5}{16\pi} \frac{m_\pi^4}{M} \log m_\pi^2 \right), \quad (31b)$$

$$\Sigma'_{\text{ET}}{}^{(++)\text{LNA}} = -\frac{3g_A^2}{32\pi f_\pi^2} \left( \frac{1}{2\pi} M m_\pi^2 \log m_\pi^2 + \frac{1}{8\pi} \frac{m_\pi^4}{M} \log m_\pi^2 \right), \quad (31c)$$

$$\Sigma'_{\text{ET}}{}^{(--)\text{LNA}} = -\frac{3g_A^2}{32\pi f_\pi^2} \left( -\frac{1}{8\pi} \frac{m_\pi^4}{M} \log m_\pi^2 \right). \quad (31d)$$

Interestingly, while LNA behavior of the positive-energy  $\Sigma'_{\text{ET}}{}^{(+ -)}$  term is  $\mathcal{O}(m_\pi^3)$ , the LNA behavior of the Z-graph  $\Sigma'_{\text{ET}}{}^{(- +)}$  actually has a lower order,  $\sim m_\pi^2 \log m_\pi$ , which arises partly from the arc contribution. This cancels, however, with an analogous arc contribution to the

$\Sigma_{\text{ET}}'^{++}$  component, so that the LNA behavior of the total is identical to that in Eq. (27). It is clear, therefore, that contributions from the arc at infinity are vital if the self-energy in the original formulation (9) is to reproduce the correct behavior of  $\Sigma$  in the chiral limit. As noted above, the reduced form (10) simplifies the computation of  $\Sigma$  considerably by avoiding arc contributions altogether.

## B. Infinite Momentum Frame

The equal-time calculation allows one to track explicitly the origins of the various LNA contributions in terms of the respective time-orderings, which are otherwise obscured in a covariant calculation. The price that one pays, however, is that many more time-ordered diagrams need to be evaluated than in a covariant formulation; while four graphs for the self-energy is tractable, for other quantities, such as vertex corrections or multi-loop diagrams, the number of time orderings quickly escalates.

It was realized some time ago [31] that by viewing the system in a Lorentz-boosted frame in which the nucleon is moving along the  $+z$  direction with infinite momentum, many time-ordered diagrams which contribute in the rest frame are suppressed by powers of the nucleon momentum,  $p_z$ , as  $p_z \rightarrow \infty$ . In particular, diagrams involving backward-moving nucleons (*i.e.*, backwards in time) in intermediate states do not contribute in this limit. The infinite momentum frame (IMF) therefore provides a simplifying framework with a much reduced number of diagrams, while at the same time retaining an intuitive, probabilistic interpretation of particle production.

The self-energy of the nucleon due to pion loops, as well as vertex and wave function renormalization, was considered by Drell, Levy and Yan (DLY) [13] using a pseudoscalar  $\pi NN$  interaction. They found, however, that extreme care must be taken to correctly treat certain cases when the nucleon's momentum fraction carried by the pion takes its limiting values of 0 or 1, and that naive application of TOPT rules in the IMF can lead to important contributions to integrals being omitted. Here we perform an analogous treatment of the self-energy for the pseudovector case, and illustrate how so-called “treacherous” points can be avoided.

We begin with the reduced form of the self-energy in Eq. (10). For the  $1/D_\pi D_N$  term, the integral over the energy  $k_0$  can be decomposed into four contributions as in Eq. (21).

For the positive energy term,  $\Sigma_{\text{IMF}}^{(+-)}$ , with the pion pole taken in the lower half-plane and nucleon pole in the upper half-plane, we parametrize the initial nucleon momentum  $p$  and intermediate nucleon and pion momenta  $p'$  and  $k$  by [13]

$$\begin{aligned} p &= (E; \mathbf{0}_\perp, P), & E &= P + \frac{M^2}{2P} + \mathcal{O}(1/P^2), \\ p' &= (E'; -\mathbf{k}_\perp, yP), & E' &= |y|P + \frac{M^2 + k_\perp^2}{2|y|P} + \mathcal{O}(1/P^2), \\ k &= (\omega_k; \mathbf{k}_\perp, (1-y)P), & \omega_k &= |1-y|P + \frac{m_\pi^2 + k_\perp^2}{2|1-y|P} + \mathcal{O}(1/P^2), \end{aligned} \quad (32)$$

where  $P \equiv p_z \rightarrow \infty$  is the nucleon's longitudinal momentum, and  $y$  is the longitudinal momentum fraction carried by the intermediate nucleon. The parametrization (32) respects the momentum conservation condition  $\mathbf{p} = \mathbf{p}' + \mathbf{k}$ . The contribution to the self-energy can then be written

$$\Sigma_{\text{IMF}}^{(+-)} = -\frac{3g_A^2 M}{16\pi^3 f_\pi^2} \int_{-\infty}^{\infty} dy \int d^2 \mathbf{k}_\perp \frac{P}{2E'} \frac{1}{2\omega_k} \frac{m_\pi^2}{(E - E' - \omega_k)}, \quad (33)$$

where we have changed the variable of integration from  $k_z$  to  $y$ . As we have already shown in the rest frame calculation in Sec. IV A, the contributions from the arc at infinity to the  $k_0$  integration of the  $1/D_\pi D_N$  term are  $\mathcal{O}(1/R_\infty)$  due to the absence of loop momenta in the numerator and the quadratic dependence on  $k_0$  in the denominator. Only pole terms contribute, therefore, to the integral over  $1/D_\pi D_N$ .

For the  $y$  integration we need to consider three regions:  $y < 0$ ,  $0 < y < 1$  and  $y > 1$ . For  $y < 0$ , which corresponds to the intermediate nucleon moving backward (in space), from the momenta parametrizations in Eq. (32) the energy denominator in Eq. (33) is

$$E - E' - \omega_k = 2yP + \mathcal{O}(1/P) \quad (y < 0). \quad (34)$$

Counting powers of the large momentum  $P$ , one sees that the integral vanishes as  $P \rightarrow \infty$ . In the region  $0 < y < 1$  the energy denominator becomes

$$E - E' - \omega_k = -\frac{k_\perp^2 + M^2(1-y)^2 + m_\pi^2 y}{2y(1-y)P} \quad (0 < y < 1), \quad (35)$$

which yields a nonzero contribution to (33) in the limit  $P \rightarrow \infty$ . Finally, when  $y > 1$ , which corresponds to the pion moving backward, one has

$$E - E' - \omega_k = 2(1-y)P + \mathcal{O}(1/P) \quad (y > 1), \quad (36)$$

which again gives a suppressed contribution as  $P \rightarrow \infty$ . Thus the only nonzero contribution is from the diagram where both the nucleon and pion are forward moving, *i.e.*,  $y > 0$  and  $1 - y > 0$ , in which case the self-energy for the positive energy diagram is

$$\Sigma_{\text{IMF}}^{(+ -)} = \frac{3g_A^2 M}{32\pi^2 f_\pi^2} \int_0^1 dy \int_0^{\Lambda_\perp^2} dk_\perp^2 \frac{m_\pi^2}{k_\perp^2 + M^2(1-y)^2 + m_\pi^2 y}, \quad (37)$$

where an ultraviolet cut-off  $\Lambda_\perp$  is introduced to regulate the  $k_\perp$  integration.

For the Z-graph, the intermediate nucleon and pion momenta are parametrized according to [13]

$$p' = (E'; \mathbf{k}_\perp, -yP), \quad k = (\omega_k; -\mathbf{k}_\perp, -(1-y)P), \quad (38)$$

satisfying the momentum conservation condition  $\mathbf{p} + \mathbf{p}' + \mathbf{k} = 0$ . The contribution to the self-energy is then given by

$$\Sigma_{\text{IMF}}^{(- +)} = \frac{3g_A^2 M}{16\pi^3 f_\pi^2} \int_{-\infty}^{\infty} dy \int d^2 \mathbf{k}_\perp \frac{P}{2E'} \frac{1}{2\omega_k} \frac{m_\pi^2}{(E + E' + \omega_k)}, \quad (39)$$

where again arc contributions at infinity are suppressed. Unlike for the  $\Sigma_{\text{IMF}}^{(+ -)}$  case above, however, since each of the  $\mathcal{O}(P)$  terms in the energy denominator add, the sum  $E + E' + \omega_k = \mathcal{O}(P)$  for all  $y$ . Counting the large momentum factors in Eq. (39) reveals that the Z-graph contribution to the self-energy is

$$\Sigma_{\text{IMF}}^{(- +)} = \mathcal{O}(1/P^2), \quad (40)$$

and thus vanishes in the limit  $P \rightarrow \infty$ . Moreover, since there are no arc contributions for the  $1/D_\pi D_N$  term in the equal-time dynamics, the terms with both poles in the upper or lower half-plane will be zero,  $\Sigma_{\text{IMF}}^{(++)} = \Sigma_{\text{IMF}}^{(--)} = 0$ , as for the rest frame calculation in Eq. (23).

For the  $1/D_N$  nucleon tadpole term in Eq. (10), the integration can be performed in an analogous way, using the parametrization of the momenta as in Eq. (32). Although it does not contain nonanalytic structure in  $m_\pi$ , it is still instructive to examine its computation in the IMF, and to demonstrate the equivalence of the results with those of the formalisms. Using the fact that the integrand is symmetric in  $y \rightarrow -y$ , the integral of  $1/D_N$  can be written

$$\int d^4 k \frac{1}{D_N} = -2\pi^2 i \int_0^\infty dy \int_0^{\Lambda_\perp^2} dk_\perp^2 \frac{1}{\sqrt{y^2 + (M^2 + k_\perp^2)/P^2}}, \quad (41)$$

where  $\Lambda_\perp$  cuts off the large transverse momenta in the  $k_\perp$  integration. After integrating over  $k_\perp$ , we note that because of the simpler structure of the denominator, we need only consider

a single region of  $y$  integration. Since the  $y$  integration is also divergent, we introduce a large- $y$  cut-off parameter,  $\lambda$ ,

$$\int d^4k \frac{1}{D_N} = -2\pi^2 i \left( \frac{\Lambda_\perp^2}{2} + \Lambda_\perp^2 \log \frac{2\lambda P}{\Lambda_\perp} + M^2 \log \frac{M}{\Lambda_\perp} \right), \quad (42)$$

with  $\lambda \rightarrow \infty$ . One could also perform the  $y$  integration first, as in DLY [13] for the pseudoscalar model, which yields the same results.

Combining the  $\pi N$  loop diagram with the nucleon tadpole, the total self-energy in the IMF can be written

$$\begin{aligned} \Sigma_{\text{IMF}} = & -\frac{3g_A^2 M}{32\pi^2 f_\pi^2} \left\{ \Lambda_\perp^2 \left( 1 + \log \frac{4\lambda^2 P^2}{\Lambda_\perp^2} \right) - 2m_\pi^2 + (M^2 + m_\pi^2) \log \frac{M^2}{\Lambda_\perp^2} \right. \\ & + \frac{m_\pi^3 \sqrt{4M^2 - m_\pi^2}}{M^2} \left( \tan^{-1} \frac{m_\pi}{\sqrt{4M^2 - m_\pi^2}} + \tan^{-1} \frac{2M^2 - m_\pi^2}{m_\pi \sqrt{4M^2 - m_\pi^2}} \right) \\ & \left. + \frac{m_\pi^4}{2M^2} \log \frac{m_\pi^2}{M^2} \right\}, \end{aligned} \quad (43)$$

which is identical to the rest frame expression (26) in its nonanalytic structure. Expanding in  $m_\pi$  then gives the LNA behavior of the self-energy in the IMF, which arises solely from the positive energy  $\pi N$  loop contribution,

$$\Sigma_{\text{IMF}}^{\text{LNA}} = \Sigma_{\text{IMF}}^{(+-)\text{LNA}} = -\frac{3g_A^2}{32\pi f_\pi^2} \left( m_\pi^3 + \frac{1}{2\pi} \frac{m_\pi^4}{M} \log m_\pi^2 + \mathcal{O}(m_\pi^5) \right). \quad (44)$$

The results differ, not surprisingly, from those of DLY [13] for the pseudoscalar  $\pi N$  interaction. In that case the calculation is performed using the original expression for  $\Sigma$  in Eq. (A3) below, where the presence of loop momenta in the numerator means that the main contribution to the self-energy arises from the infinitesimal end-point regions  $-\epsilon < y < \epsilon$  and  $1 - \epsilon < y < 1 + \epsilon$  [13] (see Appendix A). For the more consistent pseudovector theory, working with the reduced form (10) allows one to avoid this problem.

## V. LIGHT-FRONT DYNAMICS

A formalism which is similar to TOPT in the IMF is light-front, where the fields are quantized along the light-cone,  $(ct)^2 - z^2 = 0$ . The advantage of this formulation is that, as with the IMF in equal-time, many diagrams are suppressed, but the suppression is realized in any reference frame. However, as also in the IMF calculation, care needs to be taken



to correctly include contributions from end-point regions corresponding to pion light-front momentum fractions equal to 0 or 1.

We define four-momenta on the light-front as  $v = (v^+, v^-, \mathbf{v}_\perp)$ , with the plus/minus components  $v^\pm = v_0 \pm v_z$ . Note that particles on the light-front are on their mass shells, while the minus components of momenta are not conserved at vertices. In terms of light-front variables, the self-energy in Eq. (10) can be written as

$$\Sigma_{\text{LF}} = -\frac{3ig_A^2 M}{4f_\pi^2} \frac{1}{(2\pi)^4} \int dk^+ dk^- d^2 \mathbf{k}_\perp \left( \frac{m_\pi^2}{D_\pi D_N} + \frac{1}{D_N} \right), \quad (45)$$

where we have dropped the term odd in  $k$ .

Choosing the  $\mathbf{p}_\perp = 0$  frame, and performing the  $k^-$  integration, the integral of the  $1/D_\pi D_N$  term can be written

$$\begin{aligned} \int dk^+ dk^- d^2 \mathbf{k}_\perp \frac{1}{D_\pi D_N} &= \frac{1}{p^+} \int_{-\infty}^{\infty} \frac{dx}{x(x-1)} d^2 \mathbf{k}_\perp \\ &\quad \times \int dk^- \left( k^- - \frac{k_\perp^2 + m_\pi^2}{xp^+} + \frac{i\epsilon}{xp^+} \right)^{-1} \\ &\quad \times \left( k^- - \frac{M^2}{p^+} - \frac{k_\perp^2 + M^2}{(x-1)p^+} + \frac{i\epsilon}{(x-1)p^+} \right)^{-1} \\ &= 2\pi^2 i \int_0^1 dx \, dk_\perp^2 \frac{1}{k_\perp^2 + (1-x)m_\pi^2 + x^2 M^2}, \end{aligned} \quad (46)$$

where  $x = k^+/p^+$  is the plus momentum fraction of the nucleon carried by the pion. There is no arc contribution here due to the quadratic  $k^-$  dependence in the denominator. Thus, for the region  $x < 0$  or  $x > 1$ , where both poles of  $k^-$  are located either in the lower or upper half plane, respectively, the integral of  $1/D_\pi D_N$  vanishes. Consequently, only the region  $0 < x < 1$  contributes to the integration. Note that the result in (46) is identical to the IMF result for  $\Sigma_{\text{IMF}}^{(+)}$  in Eq. (37), provided the  $k_\perp$  integration is regulated by the same high-momentum cut-off  $\Lambda_\perp$  as in (37).

For the  $1/D_N$  term care needs to be taken in computing the arc contribution because of the dependence on  $k^+$  in the pole of  $k^-$ . Namely, the  $k^-$  pole is moving as  $k^+$  changes, which leads to a treacherous point as has been discussed previously in the literature [18, 19, 21, 32, 33, 34]. To see this point we can change the integration variable  $k - p \rightarrow k$  and rewrite the  $1/D_N$  term as

$$\begin{aligned} \int d^4 k \frac{1}{D_N} &= \int d^4 k \frac{1}{k^2 - M^2 + i\epsilon} \\ &= \frac{1}{2} \int d^2 \mathbf{k}_\perp \int \frac{dk^+}{k^+} \int dk^- \left( k^- - \frac{k_\perp^2 + M^2}{k^+} + \frac{i\epsilon}{k^+} \right)^{-1}. \end{aligned} \quad (47)$$

Note here that the  $k^-$  pole (*i.e.*,  $k^- = (k_\perp^2 + M^2)/k^+ - i\epsilon/k^+$ ) depends on  $k^+$ . Not only does the position of the pole depend on the sign of  $k^+$ , but also the pole moves to infinity as  $k^+ \rightarrow 0$ , changing the degree of divergence of the  $k^-$  integral from logarithmic to linear. At the point  $k^+ = 0$  the  $k^-$  integral is linearly divergent, not logarithmically divergent as one would naively expect from Eq. (47) for the  $k^+ > 0$  and  $k^+ < 0$  regions. The computation of the  $1/D_N$  term is thus highly nontrivial in light-front dynamics.

The details of this treacherous point have been discussed by Bakker *et al.* [18]. Following Ref. [18], we use the light-front cylindrical coordinates ( $k^+ = r \cos \phi$ ,  $k^- = r \sin \phi$ ) to perform the  $k^+$  and  $k^-$  integration as follows:

$$\begin{aligned} \int dk^+ dk^- \frac{1}{k^+ k^- - k_\perp^2 - M^2 + i\epsilon} &= \int_0^\infty dr \, r \int_0^{2\pi} d\phi \, (r^2 \sin \phi \cos \phi - k_\perp^2 - M^2 + i\epsilon)^{-1} \\ &= -4\pi \left[ \int_0^{r_0} dr \frac{r}{\sqrt{r_0^4 - r^4}} + i \lim_{R \rightarrow \infty} \int_{r_0}^R dr \frac{r}{\sqrt{r^4 - r_0^4}} \right] \\ &= \lim_{R \rightarrow \infty} \left( -\pi^2 + 2\pi i \log \frac{r_0^2}{R^2} + \mathcal{O}(1/R^4) \right), \end{aligned} \quad (48)$$

where  $r_0 = \sqrt{2(k_\perp^2 + M^2)}$ . The result contains the same  $\log(k_\perp^2 + M^2)$  term in the integrand as in the IMF calculation above. The  $k_\perp$  integration is then straightforward, and adding the two terms in Eq. (45) gives the total light-front self-energy

$$\begin{aligned} \Sigma_{\text{LF}} &= -\frac{3g_A^2 M}{32\pi^2 f_\pi^2} \left\{ \Lambda_\perp^2 + m_\pi^2 \log \frac{M^2}{\Lambda_\perp^2} - M^2 \log \left( 1 + \frac{\Lambda_\perp^2}{M^2} \right) - \Lambda_\perp^2 \log \left( \frac{\Lambda_\perp^2 + M^2}{R^2 e^{-i\pi/2}} \right) \right. \\ &\quad + \frac{m_\pi^3 \sqrt{4M^2 - m_\pi^2}}{M^2} \left( \tan^{-1} \frac{m_\pi}{\sqrt{4M^2 - m_\pi^2}} + \tan^{-1} \frac{2M^2 - m_\pi^2}{m_\pi \sqrt{4M^2 - m_\pi^2}} \right) \\ &\quad \left. + \frac{m_\pi^4}{2M^2} \log \frac{m_\pi^2}{M^2} \right\}. \end{aligned} \quad (49)$$

The nonanalytic part of  $\Sigma_{\text{LF}}$  is identical to the results of the covariant and equal-time (rest frame and IMF) calculations,

$$\Sigma_{\text{LF}}^{\text{LNA}} = -\frac{3g_A^2}{32\pi f_\pi^2} \left( m_\pi^3 + \frac{1}{2\pi} \frac{m_\pi^4}{M} \log m_\pi^2 + \mathcal{O}(m_\pi^5) \right), \quad (50)$$

demonstrating the equivalence of the light-front formalisms to the equal time and covariant formulations.

## VI. CONCLUSIONS

We have demonstrated the equivalence of the covariant, equal-time (both in the rest frame and the IMF), and light-front formalisms in computing the renormalization of the bare nucleon by pion loops. As a specific example, we have focussed on the self-energy of the nucleon, which finds applications in computations of pion cloud corrections to deep inelastic structure functions, form factors, and other observables. While this equivalence is expected, it has not to our knowledge been demonstrated explicitly in the literature. The calculations involve some non-trivial aspects, especially in the IMF and LF formulations, which require special care when dealing with end-point singularities, corresponding to momentum fractions approaching 0 or 1.

We focused on the chirally preferred case of pseudovector coupling, although the comparison with pseudoscalar coupling (discussed in Appendix A), which was employed in the classical work of Drell, Levy and Yan (DLY), reveals several interesting features. The leading nonanalytic behavior of the self-energy in the latter case is incorrect, with a term behaving as  $m_\pi^2 \ln m_\pi$ . In addition, whereas in the pseudovector case the scalar and vector pieces are equal and have the same LNA behavior, in the pseudoscalar theory they have even lower order (incorrect) nonanalytic terms of order  $m_\pi$ , which cancel in the full combination  $M\Sigma_v + \Sigma_s$ . Finally, we note that the technical problems encountered by DLY, with critical contributions from the regions  $-\epsilon < x < \epsilon$  and  $1 - \epsilon < x < 1 + \epsilon$ , are peculiar to the pseudoscalar case in the light-front formalism.

There are a number of applications of the methodology developed here which will be important to pursue in future. As well as the LNA behavior of the vertex renormalization,  $Z_1$ , it is important to compute the LNA behavior of the moments of the twist-two parton distribution functions. In particular, one will be able to explore within the LF formalism the results obtained by DLY [13] in the IMF, as well as the application to this problem of effective field theory [11, 15]. This should permit a satisfactory resolution of the discrepancy between the results of IMF and rest frame equal-time calculations cited by Chen and Ji [15]. It will also pave the way for a consistent interpretation of the physics of the pion cloud at the partonic level and for the development of realistic chiral models of hadron structure on the LF suitable for discussing form factors, parton distribution functions and GPDs.

## **Acknowledgements**

This work was supported by the DOE contract No. DE-AC05-06OR23177, under which Jefferson Science Associates, LLC operates Jefferson Lab. We acknowledge partial support from the Triangle Nuclear Theory fund and the NCSU theory group fund (DOE contract No. DE-FG02-03ER41260)

## APPENDIX A: SELF-ENERGY FOR THE PSEUDOSCALAR THEORY

Although the pseudoscalar Lagrangian is not invariant under chiral transformations without the introduction of a scalar field (as in the linear sigma model, for example [36]), since this theory is often discussed in the literature, for completeness we discuss here the results for the PS theory. This also allows us to contrast a number of important features pertinent to the pseudovector and pseudoscalar calculations.

The lowest order Lagrangian density for a PS  $\pi N$  interaction relevant for the self-energy is given by

$$\mathcal{L}^{\text{PS}} = -g_{\pi NN} (\bar{\psi}_N i\gamma_5 \vec{\tau} \psi_N) \cdot \vec{\phi}_\pi, \quad (\text{A1})$$

where  $g_{\pi NN}^2/4\pi \approx 14.3$  is the PS coupling constant. For on-shell nucleons obeying the free Dirac equation the PS and PV Lagrangians (see Eq. (1)) give identical results for matrix elements, provided the couplings are related by Eq. (2). For bound or off-shell nucleons, the PS and PV interactions lead to different results. However, the couplings  $f_{\pi NN}$  and  $g_{\pi NN}$  are still related through Eq. (2) since these are defined at the nucleon (and pion) poles.

The self-energy operator for the PS coupling is given by

$$\hat{\Sigma}^{\text{PS}} = i g_{\pi NN}^2 \int \frac{d^4 k}{(2\pi)^4} (\gamma_5 \vec{\tau}) \frac{i (\not{p} - \not{k} + M)}{(p-k)^2 - M^2 + i\epsilon} (\gamma_5 \vec{\tau}) \frac{i}{k^2 - m_\pi^2 + i\epsilon}. \quad (\text{A2})$$

Taking the spin trace and using Eq. (7) to replace the momentum dependence in the numerator by the nucleon and pion propagators gives for the self-energy

$$\Sigma^{\text{PS}} = -3ig_{\pi NN}^2 \int \frac{d^4 k}{(2\pi)^4} \frac{1}{2M} \frac{2p \cdot k}{D_\pi D_N} \quad (\text{A3})$$

$$= -\frac{3ig_A^2 M}{2f_\pi^2} \int \frac{d^4 k}{(2\pi)^4} \left[ \frac{m_\pi^2}{D_\pi D_N} + \frac{1}{D_N} - \frac{1}{D_\pi} \right]. \quad (\text{A4})$$

The transformed effective PS theory is represented in Fig. 2, where the self-energy now contains contributions from a scalar nucleon self-energy and a nucleon tadpole diagram, as in the PV theory, as well as a pion tadpole term.

The individual vector and scalar contributions to  $\Sigma$  are given by

$$\Sigma_v^{\text{PS}} = -3ig_{\pi NN}^2 \int \frac{d^4 k}{(2\pi)^4} \frac{M}{D_\pi D_N}, \quad (\text{A5})$$

$$\Sigma_s^{\text{PS}} = -3ig_{\pi NN}^2 \int \frac{d^4 k}{(2\pi)^4} \frac{1}{2M^2} \left[ \frac{m_\pi^2 - 2M^2}{D_\pi D_N} - \frac{1}{D_\pi} + \frac{1}{D_N} \right], \quad (\text{A6})$$

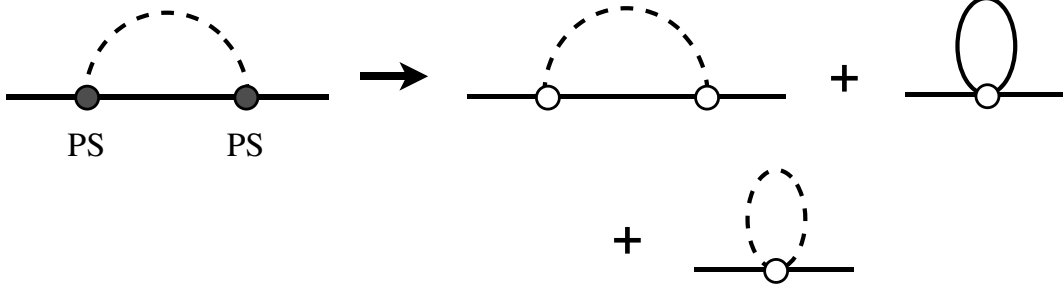


FIG. 2: Reduction of the self-energy in the pseudoscalar theory to an effective theory of “scalar nucleons” and pions (denoted by the open blobs at the vertices).

which when combined recover the full expression in Eq. (A4).

The result of the covariant calculation of the full self-energy  $\Sigma^{\text{PS}}$  using dimensional regularization is

$$\begin{aligned} \Sigma_{\text{cov}}^{\text{PS}} = & -\frac{3g_A^2 M}{32\pi^2 f_\pi^2} \left\{ \left( \gamma + \log \pi - \frac{1}{\varepsilon} + \log \frac{M^2}{\mu^2} \right) M^2 - (M^2 + m_\pi^2) \right. \\ & + \frac{m_\pi^3 \sqrt{4M^2 - m_\pi^2}}{M^2} \left( \tan^{-1} \frac{m_\pi}{\sqrt{4M^2 - m_\pi^2}} + \tan^{-1} \frac{2M^2 - m_\pi^2}{m_\pi \sqrt{4M^2 - m_\pi^2}} \right) \\ & \left. - m_\pi^2 \log \frac{m_\pi^2}{M^2} + \frac{m_\pi^4}{2M^2} \log \frac{m_\pi^2}{M^2} \right\}. \end{aligned} \quad (\text{A7})$$

Expanding in powers of  $m_\pi$ , the leading nonanalytic behavior of the self-energy in the PS theory is given by

$$\Sigma_{\text{LNA}}^{\text{PS}} = \frac{3g_A^2}{32\pi f_\pi^2} \left( \frac{M}{\pi} m_\pi^2 \log m_\pi^2 - m_\pi^3 - \frac{m_\pi^4}{2M^2} \log \frac{m_\pi^2}{M^2} + \mathcal{O}(m_\pi^5) \right). \quad (\text{A8})$$

Here the  $\mathcal{O}(m_\pi^3)$  term is identical to the leading term in the PV self-energy in Eq. (20). This is not surprising since the  $m_\pi^2/D_\pi D_N$  term in the integrand, which produces the  $m_\pi^3$  behavior, is common to both the PV and PS self-energies. However, the presence of the pion tadpole in  $\Sigma^{\text{PS}}$  (arising from the  $1/D_\pi$  term in the integrand) leads to an additional contribution proportional to  $m_\pi^2 \log m_\pi^2$ , which is of lower order than the  $m_\pi^3$  term.

Moreover, if we consider the leading nonanalytic behavior of the vector and scalar parts separately,

$$\Sigma_{v,\text{LNA}}^{\text{PS}} = \frac{3g_A^2}{32\pi f_\pi^2} \frac{1}{M} \left[ 2M^2 m_\pi + \frac{2M}{\pi} m_\pi^2 \log m_\pi^2 - m_\pi^3 + \dots \right], \quad (\text{A9})$$

$$\Sigma_{s,\text{LNA}}^{\text{PS}} = -\frac{3g_A^2}{32\pi f_\pi^2} \left[ 2M^2 m_\pi + \frac{M}{\pi} m_\pi^2 \log m_\pi^2 + \dots \right], \quad (\text{A10})$$

we find that, in contrast to the PV case, the leading order terms in both  $\Sigma_{v,\text{LNA}}^{\text{PS}}$  and  $\Sigma_{s,\text{LNA}}^{\text{PS}}$  are  $\mathcal{O}(m_\pi)$ ! While these terms cancel in the total  $\Sigma_{\text{LNA}}^{\text{PS}}$ , this demonstrates that the LNA behavior of  $\Sigma^{\text{PS}}$  is very different to that for the PV theory.

Using the original formulation as in Eq. (A3), Drell, Levy and Yan [13] computed the mass shift in the IMF formulation, finding that the entire contribution arises from the infinitesimal end-point regions  $-\epsilon < y < \epsilon$  and  $1 - \epsilon < y < 1 + \epsilon$  for the positive energy and  $Z$ -graph contributions, respectively. Moreover, the two terms separately diverge as  $P \rightarrow \infty$  or  $\epsilon \rightarrow 0$ , but the sum of the two becomes independent of  $P$  and  $\epsilon$ . While the results are ultimately the same, this illustrates the fact that the original formulation (A3) leads to a somewhat more tortuous path, at least in the IMF (and light-front) treatments than with the reduced form (A4).

## APPENDIX B: LNA BEHAVIOR OF INTEGRALS

In this appendix we summarize the leading nonanalytic behavior of various integrals which enter into calculations of the self-energy in the PV and PS theories. The relevant integrands are ones which involve a product of pion and nucleon propagators, one pion propagator (for the pion tadpole diagram in Fig. 1), or one nucleon propagator (for the nucleon tadpole diagrams in Figs. 1 and 2).

For the product of pion and nucleon propagators, one finds leading terms of order  $m_\pi$  and  $m_\pi^2 \log m_\pi^2$ ,

$$\int d^4k \frac{m_\pi^2}{D_\pi D_N} \Big|_{\text{LNA}} = -i\pi^3 \frac{m_\pi^3}{M} \left( 1 + \frac{1}{2\pi} \frac{m_\pi}{M} \log m_\pi^2 \right) + \mathcal{O}(m_\pi^5) . \quad (\text{B1})$$

The pion tadpole diagram involves the integral over a single pion propagator, and contributes to the nonanalytic behavior only at a higher order,

$$\int d^4k \frac{1}{D_\pi} \Big|_{\text{LNA}} = -i\pi^2 m_\pi^2 \log m_\pi^2 . \quad (\text{B2})$$

Note that there are no higher order contributions in  $m_\pi$  for this term. Finally, since it is independent of the pion mass, integrals involving nucleon propagators only will give zero nonanalytic contributions,

$$\int d^4k \frac{1}{D_N^n} \Big|_{\text{LNA}} = 0 , \quad (\text{B3})$$

for any power  $n$ .

- 
- [1] A. W. Thomas, Adv. Nucl. Phys. **13**, 1 (1984).
  - [2] A. W. Thomas, Phys. Lett. B **126**, 97 (1983).
  - [3] P. Amaudraz *et al.*, Phys. Rev. Lett. **66**, 2712 (1991); M. Arneodo *et al.*, Phys. Lett. B **364**, 107 (1995).
  - [4] A. Baldit *et al.*, Phys. Lett. B **332**, 244 (1994).
  - [5] E. A. Hawker *et al.*, Phys. Rev. Lett. **80**, 3715 (1998).
  - [6] A. W. Schreiber and A. W. Thomas, Phys. Lett. B **215**, 141 (1988).
  - [7] F. Myhrer and A. W. Thomas, Phys. Lett. B **663**, 302 (2008).
  - [8] A. W. Thomas, W. Melnitchouk and F. M. Steffens, Phys. Rev. Lett. **85**, 2892 (2000).
  - [9] W. Detmold, W. Melnitchouk, J. W. Negele, D. B. Renner and A. W. Thomas, Phys. Rev. Lett. **87**, 172001 (2001).
  - [10] J.-W. Chen and X. Ji, Phys. Lett. B **523**, 107 (2001).
  - [11] D. Arndt and M. J. Savage, Nucl. Phys. A **697**, 429 (2002).
  - [12] For review see X. Ji, Ann. Rev. Nucl. Part. Sci. **54**, 413 (2004); A. V. Belitsky and A. V. Radyushkin, Phys. Rept. **418**, 1 (2005).
  - [13] S. D. Drell, D. J. Levy and T. M. Yan, Phys. Rev. D **1**, 1035 (1970).
  - [14] J.-W. Chen and X. Ji, Phys. Rev. Lett. **87**, 152002 (2001) [Erratum-ibid. **88**, 249901 (2002)].
  - [15] J.-W. Chen and X. Ji, Phys. Lett. B **523**, 73 (2001).
  - [16] W. Melnitchouk and A. W. Thomas, Phys. Rev. D **47**, 3794 (1993).
  - [17] J. Speth and A. W. Thomas, Adv. Nucl. Phys. **24**, 83 (1997).
  - [18] B. L. G. Bakker, M. A. DeWitt, C.-R. Ji and Y. Mishchenko, Phys. Rev. D **72**, 076005 (2005).
  - [19] A. Misra and S. Warawdekar, Phys. Rev. D **71**, 125011 (2005).
  - [20] M. Sawicki, Phys. Rev. D **44**, 433 (1991); Phys. Lett. B **268**, 327 (1991).
  - [21] M. Burkardt, Phys. Rev. D **57**, 1136 (1998).
  - [22] M. Burkardt, C.-R. Ji, W. Melnitchouk and A. W. Thomas, in preparation.
  - [23] See, *e.g.*, V. Bernard, N. Kaiser and U. G. Meissner, Int. J. Mod. Phys. E **4**, 193 (1995).
  - [24] T. Ericson and W. Weise, *Pions and Nuclei* (Clarendon Press, Oxford, 1988).
  - [25] M. B. Hecht, M. Oettel, C. D. Roberts, S. M. Schmidt, P. C. Tandy and A. W. Thomas, Phys. Rev. C **65**, 055204 (2002).



- [26] J. D. Bjorken and S. Drell, *Relativistic Quantum Fields* (McGraw Hill, New York, 1965).
- [27] By “scalar nucleon” we mean that there is no momentum in the numerator of the self-energy  $\Sigma$ , as in a theory of pions and spin-0 nucleons.
- [28] S. Scherer and M. R. Schindler, arXiv:hep-ph/0505265.
- [29] M. Procura, T. R. Hemmert and W. Weise, Phys. Rev. D **69**, 034505 (2004).
- [30] D. B. Leinweber, A. W. Thomas, K. Tsushima and S. V. Wright, Phys. Rev. D **61**, 074502 (2000).
- [31] S. Weinberg, Phys. Rev. **66**, 1313 (1966).
- [32] N. E. Ligterink and B. L. G. Bakker, Phys. Rev. D **52**, 5954 (1995).
- [33] H.-C. Pauli and S. J. Brodsky, Phys. Rev. D **32**, 1993 (1985).
- [34] T.-M. Yan, Phys. Rev. D **7**, 1780 (1973).
- [35] J. D. Sullivan, Phys. Rev. D **5**, 1732 (1972).
- [36] A. W. Thomas and W. Weise, *The Structure of the Nucleon*, (Wiley-VCH, Berlin, 2001).